ORIGINAL PAPER

MANNOSE - PEROXYDISULFATE REACTION: QUALITATIVE PRODUCT ANALYSIS, SURFACE EFFECT AND EXPERIMENTAL KINETIC MEASUREMENTS

MUSTAFA J.A. ABUALREISH[1]

Manuscript received: 06.07.2024; Accepted paper: 23.08.2024;
Published online: 30.09.2024.

Abstract. *Peroxydisulfate (PDS) is a powerful oxidizing agent for reducing sugars. Throughout the redox interaction with the D(+)mannose molecule, the current work used the iodometric technique of measurement to track the unconsumed (PDS) at various time intervals. The existence of formaldehyde and formic acid in the qualitative test of the volatile redox reaction products suggests that the mannose molecule undergoes oxidative cleavage at its C-C bonds and the aldehydic and primary alcoholic groups. According to surface effect experiments, the redox reaction is characterized by chain reactions. Based on the results of the kinetics experiments, it was determined that the reaction rate is first order for [PDS] and fractional order for [Mannose] and that both respond more rapidly as the concentrations of these substances rise. Investigating the effect of temperature on the redox reaction under controlled experimental settings revealed that increasing the temperature resulted in a faster pace. The activation energy of the redox process was calculated to be 26.85 kcal/mole based on the oxidation rate measurements taken at different temperatures. Other activation functions, such as the frequency factor, the change in free energy, and the change in entropy, were also measured at different temperatures. A rate law was developed, and appropriate reaction pathways for the oxidation of D(+)mannose were proposed based on the collected experimental data...*

Keywords: *peroxydisulfate; D(+)Mannose; iodometric method; qualitative analysis; surface effect; activation functions.*

1. INTRODUCTION

Research into the bio and physiochemical characteristics and reactivities of carbohydrates, particularly mono- and di-saccharides, has proven very reliable from a biological and economic perspective [1-7]. The redox behavior of carbohydrates plays a significant role in their microbiological and physiological activities [8, 9]. Various oxidants may cause sugars to undergo oxidation, and this phenomenon has been extensively studied in the literature [10-16]. Much study has focused on the oxidation of sugars, particularly mono- and disaccharides [17-33]. A large variety of organic molecules may be oxidized by peroxydisulfate, either directly or indirectly, via the radical intermediates [34]. The chemistry and uses of oxidation systems based on peroxydisulfate have been explored in several studies in the last few years [35-40]. Peroxydisulfate activation to destroy the target compound has been demonstrated to be obtainable using thermal [41] or chemical activation by transition metals [42-43]. It has been demonstrated that sodium peroxydisulfate ($Na_2S_2O_8$) can break down stable molecules by facilitating the production of sulfate free radicals ($SO^{\cdot}_4$) when

[1] Northern Border University, College of Science, Department of Chemistry, Arar, Saudi Arabia.
E-mail: Mustafa.Abualreish@nbu.edu.sa.

https://doi.org/10.46939/J.Sci.Arts-24.3-b02

activated [44-45]. The free radical sulfate, which has a redox potential [$SO_4^{\cdot}/SO_4^{2-}$] of 2.6 V) [46] is an oxidizing agent that is more active than peroxydisulfate anion (E^o [$S_2O_8^{2-}/ 2SO_4^{2-}$] of 2.01 V) [47]. This work is significant because no previous research has documented a thorough examination of the kinetics of the uncatalyzed reaction of mannose with peroxydisulfate, wherein the compounds generated during oxidation are treated to understand the mechanism and construct a rate law. The current research aims to learn more about the redox reaction mechanism, build a rate law, and assess the efficacy of using activated peroxydisulfate to oxidize mannose.

2. MATERIALS AND METHODS

2.1. MATERIALS

Chemicals were ordered from well-known supply sources such as Scarlab. S.L., Spain and Acrös, USA. Analytical grade potassium peroxydisulfate (PPDS) ($K_2S_2O_8$, 99%) and D(+)Mannose ($C_6H_{12}O_6$, 99%) were purchased from Acrös, USA, and used without further purification in their original form. Sulfuric acid sodium ($Na_2S_2O_3$, 98%), sulfuric acid (H_2SO_4, 95-98%), sodium hydrogen carbonate ($NaHCO_3$, 99%), potassium iodide (KI, 99%), and Starch (soluble) were purchased from Scarlab. S.L., Spain, and used as received without further purification. According to the standard analytical procedures, deionized water was used to prepare aqueous solutions used in all experiments.

2.2. METHODS

2.2.1. Determination of Peroxydisulfate Concentration [PDS]

According to what has been published, $S_2O_8^{2-}$ (peroxydisulfate) may be determined in many ways. Iodometry [48–50], ferrometry [51–54], and the polarographic technique [55,56] are some of the more conventional approaches. Electrochemiluminescence (ECL) [57–63], electrochemical technique [64–67], UV-VIS spectrophotometry [68–70], fluorescence method [71,72], resonant Rayleigh scattering (RRS) method [73], and liquid chromatography (LC) [74–78] are some of the newly developed methods. The detection limits, execution times, accuracy, and sensitivity of these approaches differ.

2.2.2. Iodometric method to determine the unconsumed [PPDS] during the redox reaction

As the redox interaction between PPDS and D(+)mannose is not detectable at ambient temperature (t 1/ 2 = one month) [79], temperatures between 60 and 80 °C were used [80]. To achieve thermal equilibrium in this experiment, the reaction vessel was filled with the correct volume of distilled water and D(+)mannose solution (enough to maintain a total capacity of 100 mL volumetric flask for all runs). The temperature was then thermostated. The reaction mixture was swiftly supplemented with a thermostated PPDS solution that had been transferred separately. For iodometric monitoring of the reaction process, 5 mL aliquots of the reaction mixture were pipetted into conical flasks at various time intervals. These flasks were then filled with 5 mL of 4% $NaHCO_3$, 1 mL of 1N H_2SO_4, and 5 mL of 30% KI (typically

newly made). At the endpoint (color disappearance), starch was used as an internal indicator to titrate the freed iodine against a standard solution of 0.1 M sodium thiosulfate.

2.2.3. Qualitative analysis of the redox reaction products

For five days at 60°C, a solution of 25 grams of D(+)mannose and 25 g of potassium peroxydisulfate in 250 mL of water was refluxed until the peroxydisulfate was completely consumed. For this purpose, a reflux condenser was used, which included the circulation of cold water during the heating process to keep the volatile chemicals from escaping. The reaction mixture was obtained once the reflux was complete and fractionally separated into volatile and nonvolatile products.

Formaldehyde. In a test tube, 2 mL of concentrated sulfuric acid and 2 mL of chromotropic acid were added to 0.5 mL of the remaining distillate. A water bath was used to heat the mixture to 60°C for 10 minutes. By adding 2,4-dinitrophenylhydrazine to the portion of distillate and recrystallizing it from ethanol, a 2,4-dinitrophenylhydrazine derivative of formaldehyde was synthesized to validate its existence.

Formic Acid. 2 mL of the distillate combined with 1 mL of $HgCl_2$ solution and the mixture was heated. By combining 2 mL of the mixture with 1 gram of PCl in a porcelain vessel, the amide derivative of formic acid was created to validate its existence. After the ingredients were combined to a liquid state, 20 mL of NH_4OH solution was added gradually. After that filtered, cold water was used to wash the mixture. Drying and recrystallization of the derivative from water

2.2.4. Surface Effect

It was necessary to conduct experiments to evaluate the following to determine the surface influence on the mannose-peroxy disulfate reaction. *The methods of cleaning the reaction vessel*. To test this factor few runs were done at equal concentrations of mannose and peroxydisulfate of 0.02M and 60°C. Step one included washing the 500 mL iodine flask with chromic acid and deionized water finally steaming and drying it in a 100°C oven. Second step - the vessel (same as before) was washed with soap, concentrated hydrochloric acid, and deionized water; it was then dried in an oven set at 100°C. *The effect of adding an extra surface*. In a set of kinetic runs at equal concentrations of mannose and peroxydisulfate of 0.02 M and at 60°C, known $BaSO_4$ and glass wool weights were added.

2.2.5. Kinetic measurements

a) Order of the mannose-peroxydisulfate reaction

To investigate the order of the mannose- peroxydisulfate reaction, a set of experiments at comparatively low [PDS], in which the ratio[PDS]/ [Mannose] = 0.04, were carried out.

b) Rate dependence on [PDS]

The reaction was examined at different initial concentrations of peroxydisulfate, ranging from 0.005M to 0.08M, to see if [PDS] increases, decreases, or has no impact on the pace of the redox reaction. While [Mannose] maintained constant at 0.02 M, the temperature remained constant at 60°C. The unconsumed [PDS] was followed iodometrically during the redox reaction at different time intervals.

c) Rate dependence on [Mannose]

The effect of [Mannose] was studied at different concentrations ranging from 0.002 to 0.08 M. The temperature was kept constant at 60°C.

d) The impact of temperature

It looked at the temperature dependence of the measured rate constant from 60 to 80°C. For both [PDS] and [Mannose], the trials were conducted at a concentration of 0.02 M. The temperature effect is also helpful when determining the activation energy using the Arrhenius Equation [81, 82] and other thermodynamic parameters, according to [79].

e) Thermal decomposition of peroxydisulfate

A series of studies examined the thermal breakdown of peroxydisulfate alone at 60, 70, 75, and 80°C. The concentration of peroxydisulfate was maintained at 0.02 M in these experimental setups.

f) Confirmation of the rate law at higher temperatures and evaluation of Ea for K_2

Various studies were conducted at temperatures 70, 75, and 80°C. In these trials, the peroxydisulfate concentration was constant at 0.02M, whereas the mannose concentration ranged from 0.005 M to 0.08 M.

g) Proposed Mechanism and Rate Law

The mannose-peroxydisulfate reaction resulted in the formation of formaldehyde and formic acid as volatile fractions and the non-volatile fraction was referred to as the residue which consisted mainly of potassium hydrogen sulfate, aldonic and aldaric acids along with other products of oxidation [83].

3. RESULTS AND DISCUSSION

3.1. PRODUCT QUALITATIVE ANALYSIS

Formaldehyde - When formaldehyde was present, a violet coloration emerged. Recrystallization of the prepared formaldehyde derivative from ethanol produced a melting point (m.p.) of 166-167°C, identical to that of the pure derivative [84].

Formic Acid - Formic acid was detected when a white precipitate transformed into a grey-black color. The recrystallized and dried formic acid derivative used to verify formic acid presence has a melting point between 194 and 195°C, identical to that of the pure derivative.

Surface Effect - The methods of cleaning the reaction vessel

Table 1. Reaction rate constant ko of mannose-peroxy disulfate at 60°C as a function of cleaning procedure for the reaction vessel (500 mL iodine flask).

The methods of cleaning the reaction vessel	**10^5 k_o [sec^{-1}]**
Chromic acid and deionized water were used to clean the vessel. After that, it was steamed and dried in an oven set at 100°C.	3.59
Finally, the vessel was steamed and dried in an oven at 100°C after being cleaned with soap, concentrated hydrochloric acid, and deionized water.	2.99
[PDS]$_O$ = **[Mannose]**$_O$ = 0.02 M	

There is a difference in the rate constant, which means the method of cleaning the reaction vessel has an impact on the value of the observed rate constant k_o, this supports the assumption that the mannose -peroxydisulfate reaction involved a chain mechanism.

The effect of adding an extra surface

Table 2. Surface addition's impact on the mannose-peroxydisulfate reaction's measured rate constant ko at 60°C.

Weight of added $BaSO_4$ [g]	**10^5 k_o [sec^{-1}]**
---	3.12
0.799	3.11
1.598	3.12
2.200	3.12
2.230	3.11
[PDS]$_O$ = **[Mannose]**$_O$ = 0.02 M	

There is no observable change between the different experiments but on adding 5 g of glass wool, the observed rate constant k_o increased to $5.39 \cdot 10^{-5}$ indicating that glass wool catalyzed the reaction. This result confirmed the belief that the mannose-peroxydisulfate reaction is characteristic of chain reactions. Such chains are sensitive to the nature of the reaction vessel surface.

Kinetic measurements
Order of the mannose- peroxydisulfate reaction

Table 3. Order of the mannose- peroxydisulfate reaction at 60°C.

Time [s]	**Titre [mL]**	**log [PDS]**
0	10.95	1.039
3600	9.65	0.985
7200	7.05	0.848
10800	3.65	0.562
14400	2.05	0.312
21600	0.55	-0.249
[PDS]/ [Mannose]=0.04**, [PDS]**$_O$ = 0.02 M **,[Mannose]**$_O$ = 0.5 M		

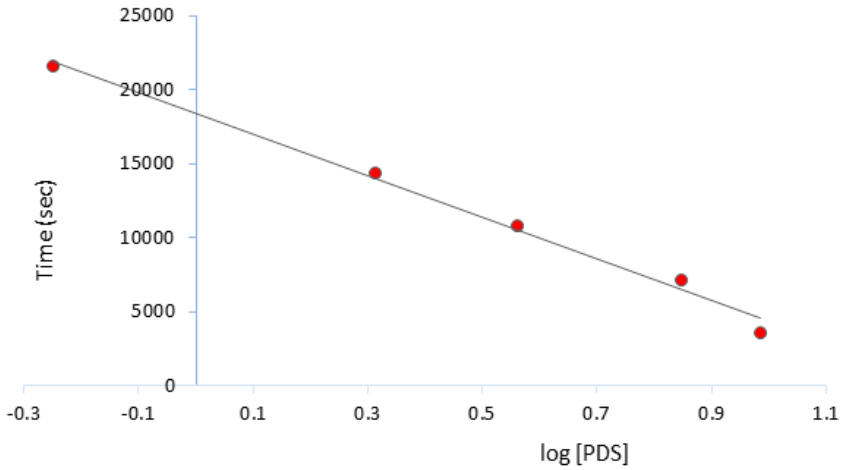

Figure 1. The plot of log [PDS] against time at 60^{O}C.

The unreacted [PDS] decreased linearly with time (Fig.1, Table 3) indicating that the mannose- peroxydisulfate reaction was first order in [PDS] satisfying the Equation (1):

$$R = k_0[PDS] \quad (1)$$

where k_O is the observed rate constant and R is the rate

Rate dependence on [PDS]

Table 4. Rate dependence on [PDS] at 60°C, $[Mannose]_O$ = 0.02 M

$10^3[PDS]_o$ M	5	10	20	30	40	50	60	80
$10^3[PDS]_{average}$ M	2.22	6.86	14.79	21.45	31.02	34.09	41.07	55.97
10^7 R [L·mol^{-1}·sec^{-1}]	1.174	2.319	3.913	6.769	7.153	8.987	10.719	15.079
10^5 k_o [sec^{-1}]	6.15	3.24	2.70	2.95	2.45	2.80	2.68	2.76

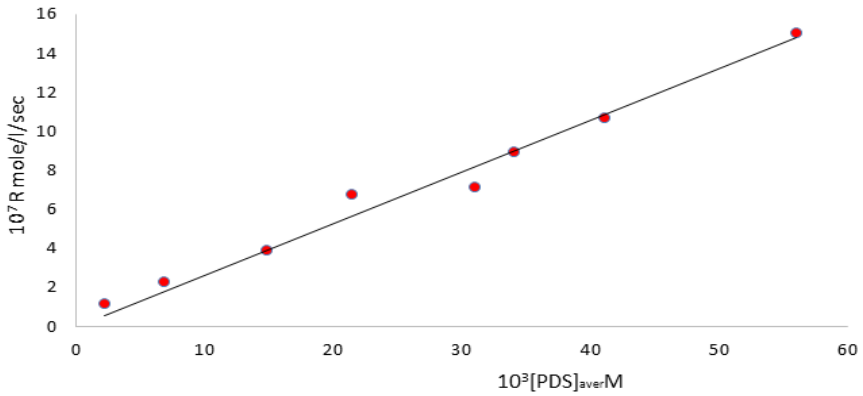

Figure 2. Rate dependence on [PDS] at 60°C

When $[PDS]_o$ was gradually raised, the rates plotted against $[PDS]_{average}$, (Fig. 2, Table 4), the relationship was linear passing through the origin at zero $[PDS]_{average}$, In Fig. 2, the value of is shown by the slope of the line $k_O = 2.65 \cdot 10^{-5}$ at 60°C for mannose-peroxydisulfate reaction. In plotting k_O the observed rate constant against the initial concentration of peroxydisulfate $[PDS]_o$, (Fig. 3, Table 4), the relationship was linear, parallel to the *x*-axis, and with intercept $2.67 \cdot 10^{-5}$.

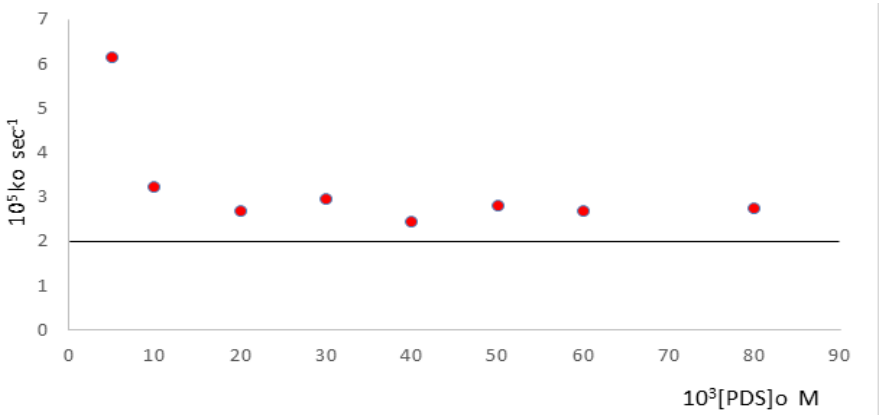

Figure 3. The plot of the observed rate constant ko against the initial concentration of peroxydisulfate [PDS]o at 60°C

Rate dependence on [Mannose]

Table 5. Rate dependence on [Mannose] at 60°C, $[PDS]_O$ = 0.02 M

10^3**[Mannose]$_o$** M	2	5	10	20	40	50	80
10^3**[$S_2O_8^{=}$]$_{aver}$** M	0.01540	0.01500	0.01480	0.01470	0.0127	0.0132	0.0140
10^6 **R** [L·mol^{-1}·sec^{-1}]	0.2800	0.3674	0.3821	0.3814	0.3915	0.3896	0.4460
10^5 **k_o** [sec^{-1}]	1.67	2.10	2.27	2.70	2.83	2.92	3.15
[Mannose]$_o^{0.2}$ M	0.2885	0.3465	0.3981	0.4634	0.5253	0.5493	0.6034

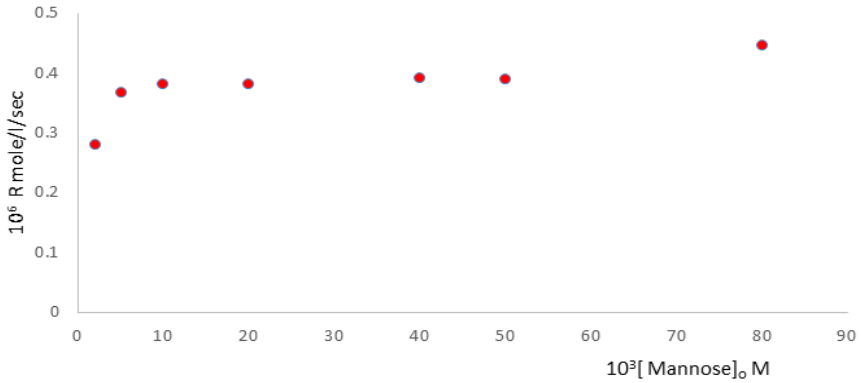

Figure 4. Plot of the rate R against [Mannose]$_o$ M at 60°C

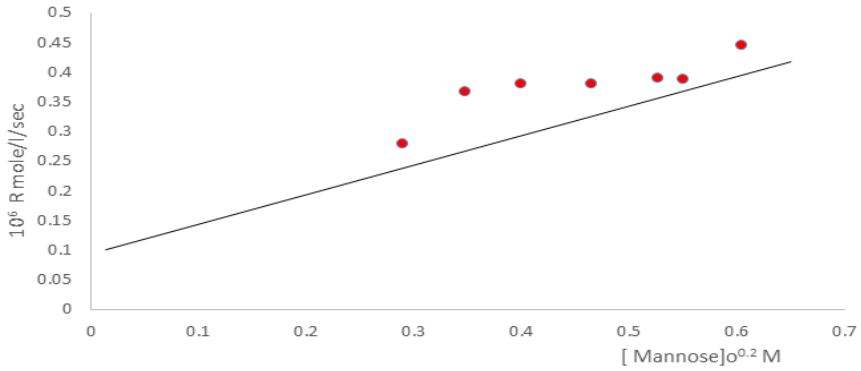

Figure 5. Plot of the rate R against [Mannose]$_o^{0.2}$ M at 60°C

From Table 5, it is clear that the rate of mannose- peroxydisulfate reaction (R) increases as [Mannose] is increased, when (R) was plotted versus [Mannose]$_O$ a curve was obtained (Fig. 4), this curve indicated that the mannose- peroxydisulfate reaction order was not unity concerning [Mannose]. Several other plots were attempted in which [Mannose] was raised to a certain power. With a power of 0.2 the plots of (R) becomes linear (Fig. 5) with [Mannose], but the line did not pass through the origin at zero concentration. The value of the intercept may be compared with $0.121 \cdot 10^{-6}$ L·mol^{-1}·sec^{-1} on the thermal breakdown of (PDS) when a reducing substrate is not present.

Based on these findings, we can write the rate of the mannose-peroxydisulfate reaction as follows:

$$R = R' + R^{=} \tag{2}$$

The rate of the mannose-peroxydisulfate reaction is denoted by R; R' is the rate of thermal decomposition of peroxydisulfate alone; $R^{=}$ is the rate term which corresponds to the bimolecular reaction between mannose and peroxydisulfate and takes the form:

$$(K_2[PDS][Mannose]^{0.2})$$

Equation (2) shows that the rate law for mannose – peroxydisulfate reaction consists of at least two terms, one represents the decomposition of peroxydisulfate alone and the other term represents the bimolecular reaction between mannose and peroxydisulfate. Therefore, suggest the following rate law for these reactions:

$$R = K_1[PDS] + K_2[PDS][Mannose]^{0.2} \tag{3}$$

The above equation when integrated gave the following relationship:

$$k_o = K_1 + K_2[\text{Mannose}]^{0.2} \quad (4)$$

where k_o denoted the rate constant observed for the mannose-peroxydisulfate reaction; K_1 denoted the rate constant of the isolated peroxydisulfate thermal decomposition; K_2 is the rate constant of the bimolecular reaction between mannose and peroxydisulfate.

In Equation (4) k_o and K_1 were determined experimentally but K_2 cannot be directly determined, it can only be determined from the graph. To verify Equation (4), k_o values from Table 5 were plotted against $[\text{mannose}]^{0.2}$, the illustration showed a straight line (Fig. 6), and the line's intercept equal $0.468 \cdot 10^{-5}$ sec^{-1} at zero mannose concentration. This value compares well with the value of K_1 obtained from the thermal decomposition of peroxydisulfate alone at the same temperature ($K_1 = 0.47 \cdot 10^{-5} sec^{-1}$) Table 10.

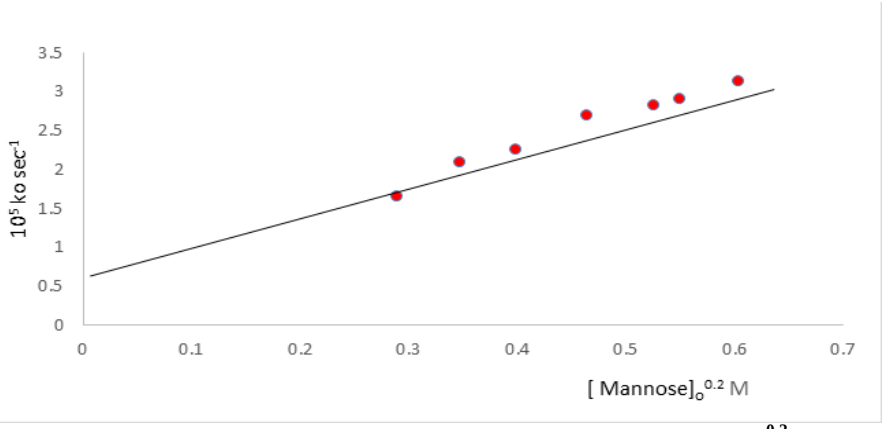

Figure 6. The plot of the observed rate constant ko against $[\text{Mannose}]_o^{0.2}$ M at 60°C

The linearity obtained in Fig. 6 and the value of the intercept being the same as that of peroxydisulfate alone, both verify Equation (4) and thus can be used to confirm the order of the reaction in mannose concentration. A slightly altered variant of Equation (3) may be expressed as follows:

$$R = R' + K_2[\text{PDS}][\text{Mannose}]^n \quad (5)$$

or

$$\frac{R - R'}{[\text{PDS}]} = K_2[\text{Mannose}]^n \quad (6)$$

Taking the logarithm of the equation was obtained :

$$\log\frac{R - R'}{[\text{PDS}]} = \log K_2 + n\log[\text{Mannose}] \quad (7)$$

Table 6. The values of log R-R'/[PDS] and log [Mannose] at temp.=60°C

10^3**[PDS]$_{aver}$** M	0.01540	0.01500	0.01480	0.01470	0.0127	0.0132	0.0140
10^3**[Mannose]$_o$** M	2	5	10	20	40	50	80
3+log **[Mannose]$_o$**	0.3010	0.6990	1.0000	1.3010	1.6021	1.6990	1.9031
10^6 **R**	0.2800	0.3674	0.3821	0.3814	0.3915	0.3896	0.4460
10^6 **[R-R']**/10^3**[PDS]$_{aver}$**	10.3246	16.4267	17.6419	17.7143	21.2992	20.3485	23.2143
6+ log[R-R']/[PDS]$_{aver}$	1.0139	1.2155	1.2465	1.2483	1.3284	1.3085	1.3658
$[PDS]_O$ = 0.02 M **10^6 R' = 0.121**							

The log plot R-R'/[PDS] against log [Mannose] at temp.=60°C provided the data in the form of a straight line (Fig. 7) with a slope of 0.20, thus confirming that n = 0.20 in

Equation (5). The line's intercept at log[Mannose] = O gave log K_2 from which K_2 was equal to $4.52 \cdot 10^{-5}$ L·mol^{-1}·sec^{-1} for mannose – peroxydisulfate reaction.

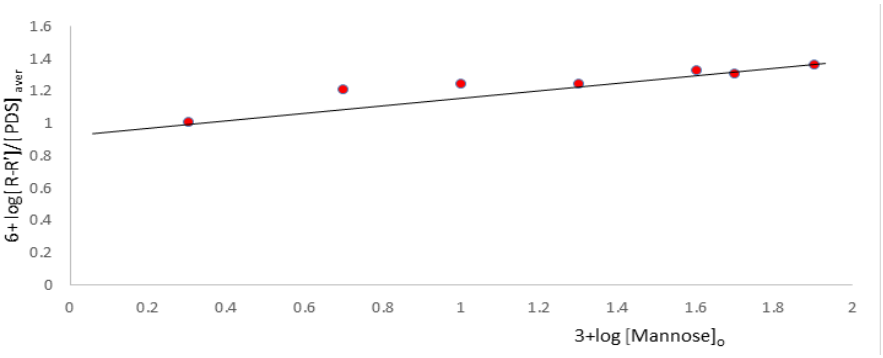

Figure 7. Plot of log R-R'/[PDS] against log [Mannose]at 60°C.

Table 7. Values of K_2 from Equation 4: $[PDS]_O$ = 0.02 M

10^3[**Mannose**]$_o$ M	2	5	10	20	40	50	60	80	10^5 **k$_2$** [L·mol^{-1}·sec^{-1}]
[**Mannose**]$_o^{0.2}$ M	0.2885	0.3465	0.3981	0.4634	0.5253	0.5493	0.5697	0.6034	
10^5 **k$_o$** sec^{-1} at 60 ^{O}C	1.67	2.10	2.27	2.70	2.83	2.92	-	3.15	4.52
10^5 **k$_o$** sec^{-1} at 70^{O}C	-	5.93	5.84	7.70	7.66	-	8.17	-	11.11
10^5 **k$_o$** sec^{-1} at 75^{O}C	-	10.04	12.70	14.47	15.31	-	15.12	17.80	17.99
10^5 **k$_o$** sec^{-1} at 80^{O}C	-	23.50	25.22	28.24	31.40	-	-	-	37.57

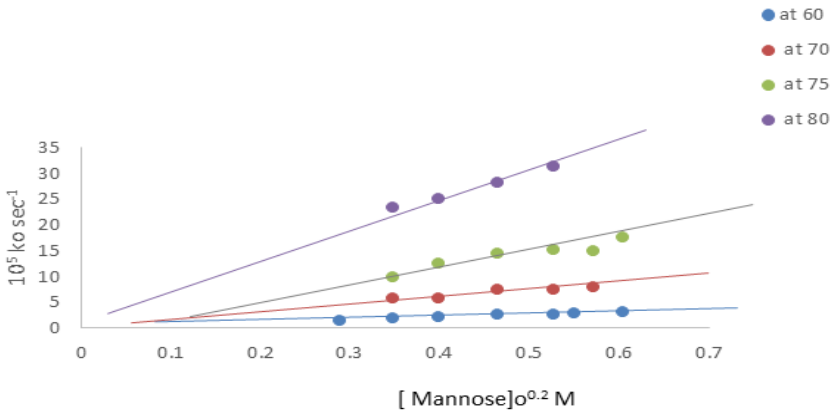

Figure 8. Confirmation of the rate law by equation 4 over the range 60-80°C.

Fig. 8 shows the plot of k_o against $[Mannose]_o^{0.2}$ M at 60, 70, 75, and 80°C. At each temperature, the intercepts of the lines show the values of k_1, the rate constant of the thermal decomposition of peroxydisulfate alone; this confirms Equation (4) and indicates that the order of the mannose-peroxydisulfate reaction with respect to mannose remains 0.2 at higher temperatures, the slopes of the plot show the values of k_2. Table 14 contains the data for each temperature.

The impact of temperature

Table 8. Rate dependence on temperature, $[PDS]_O$ =$[Mannose]_O$= 0.02 M

T [K]	10^3 1/T	10^5 k_o [sec^{-1}]	ln k_o	5 + log k_o
333	3.000	2.90	-10.448	0.4624
343	2.915	7.90	-9.446	0.8976
348	2.874	14.69	-8.826	1.1670
353	2.833	28.46	-8.164	1.4542

It is evident from Table 8 that raising the temperature accelerates the reaction rate. the plot of $1/T \cdot 10^3$ and log k_o according to Arrhenius Equation [81,84]:

$$K = exp^{-\frac{Ea}{RT}} \text{ or } \ln k = \ln A - \frac{Ea}{RT}$$

The rate constant, pre-exponential factor, activation energy, universal gas constant, and temperature are all represented by the variables k, A, Ea, R, and T, respectively. determined that the energy of activation (E_a) for the mannose-peroxydisulfate reaction was 26.85 kcal, as shown by the slope of the straight line (Fig. 9). Table 9 also includes other thermodynamic data, such as the activation entropy change ($\Delta S^{\#}$) and the activation free energy change (ΔG#) were determined using the following formulas:

$$\Delta S^{\#} = 2.303R\left(\log A - \log\frac{RT}{Nh}\right)[J \cdot K]$$
$$\Delta G^{\#} = \Delta E_a - T\Delta S^{\#}[\,kJ/mol]$$

where R/N is Boltzmann's gas constant $1.3806 \cdot 10^{-23}$ $J \cdot deg^{-1}$; h is Plank's constant, $6.625 \cdot 10^{-34}$ $J \cdot s^{-1}$.

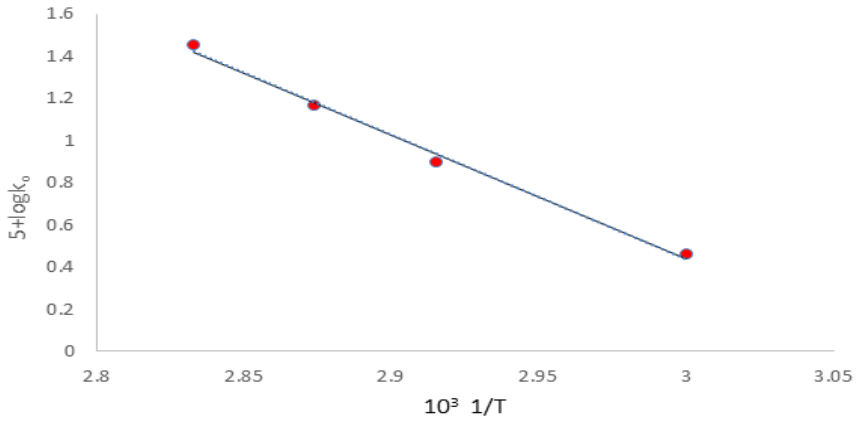

Figure 9. The impact of temperature on k_o over the range of 60-80°C.

Table 9. Thermodynamic functions for the mannose-peroxydisulfate reaction.

Activation functions	**Found**			
Energy of activation (Ea) [kcal/mol]	26.85			
Frequency factor (A), (pre-exponential factor) [sec^{-1}]	$1.6 \cdot 10^{-5}$			
The change in free energy ($\Delta G^{\#}$) [kJ/mol] at various temperatures [K]	**333**	**343**	**348**	**353**
	112.55	116.01	117.74	119.47
Entropy change ($\Delta S^{\#}$) [J/K] at different temperatures [K]	**333**	**343**	**348**	**353**
	-337.65	-337.89	-338.01	-338.13

Thermal decomposition of peroxydisulfate

Table 10. R and Ko values for peroxydisulfate thermal decomposition at 60–80°C and [PDS]O = 0.02 M.

Temperature [°C]	10^6 **R'** [$L \cdot mol^{-1} \cdot sec^{-1}$]	10^5 k_o [sec^{-1}]
60	0.121	0.47
70	0.459	1.94
75	0.668	2.14
80	1.269	7.78

Confirmation of the rate law at higher temperatures and evaluation of E_a for K_2

Table 11. The values of log R-R'/[PDS] and log[Mannose] at temp.=70°C

10^3[PDS]$_{aver}$ M	0.01409	0.01390	0.01295	0.0123	0.0091
10^3[Mannose]$_o$ M	5	10	20	40	60
3+log [Mannose]$_o$	0.6990	1.0000	1.3010	1.6021	1.7782
10^6 R	0.8309	0.80	0.973	1.0562	1.079
10^6 [R-R']/ 10^3[PDS] $_{aver}$	26.3946	24.5324	39.6911	48.5528	68.1319
6+ log[R-R'] /[PDS] $_{aver}$	1.4215	1.3897	1.5987	1.6862	1.8334
[PDS]$_O$ = 0.02 M 10^6 R' = 0.459					

Table 12. The values of log R-R'/[PDS] and log[Mannose] at temp.=75°C

10^3[PDS]$_{aver}$ M	0.01175	0.01169	0.01239	0.0099	0.011290	0.0099
10^3[Mannose]$_o$ M	5	10	20	40	60	80
3+log [Mannose]$_o$	0.6990	1.0000	1.3010	1.6021	1.7782	1.9031
10^6 R	1.2687	1.493	1.755	1.645	1.592	1.739
10^6 [R-R'] /10^3[PDS] $_{aver}$	51.1234	70.5731	87.7320	98.6869	81.8423	108.1818
6+ log[R-R'] / [PDS] $_{aver}$	1.7086	1.8486	1.9432	1.9943	1.9130	2.0342
[PDS]$_O$ = 0.02 M 10^6 R' = 0.668						

Table 13. The values of log R-R'/[PDS] and log[Mannose] at temp.=80°C

10^3[PDS]$_{aver}$ M	0.01322	0.01324	0.01269	0.01185
10^3[Mannose]$_o$ M	5	10	20	40
3+log [Mannose]$_o$	0.6990	1.0000	1.3010	1.6021
10^6 R	3.046	3.249	3.386	3.644
10^6 [R-R'] /10^3[PDS] $_{aver}$	134.4175	149.5468	166.8243	200.4219
6+ log[R-R'] / [PDS] $_{aver}$	2.12846	2.1748	2.2223	2.3019
[PDS]$_O$ = 0.02 M 10^6 R' = 1.269				

The plot of log R-R'/[PDS] against log [Mannose] over the whole temperature range investigated gave straight lines (Fig. 10), and the slopes of the lines(n) vary between 0.20-0.24 thus confirming that the order of the reaction unchanged at higher temperatures. The intercepts of the lines at zero log [Mannose]=0 in Fig.10 gave the values of log k_2 at different temperatures and k_2 values obtained by this method compared with those from Fig. 8 and are included in Table 14.

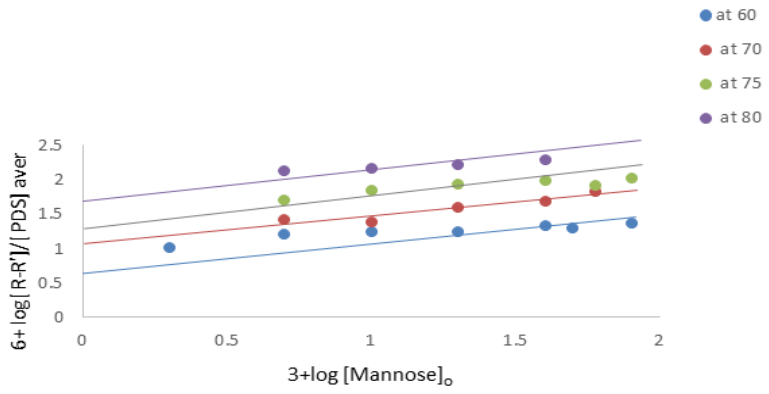

Figure 10. Confirmation of the reaction order for mannose and evaluation of k_2 from Equation 7 over the range 60-80°C.

Table 14. Dependence of k_2 and n on temperature.

Temperature [°C]	**60**	**70**	**75**	**80**
n (Fig. 10)	0.20	0.22	0.24	0.20
10^5 k_2 (Fig. 8) [L·mol^{-1}·sec^{-1}]	4.52	11.11	17.99	37.57

Temperature [°C]	60	70	75	80
10^5 k_2 (Fig. 10) [L·mol^{-1}·sec^{-1}]	4.54	10.29	14.49	34.59
Average k_2 [L·mol^{-1}·sec^{-1}]	4.53	10.70	16.24	36.08

Table 15. Evaluation of Ea for k_2: $[PDS]_O$ =$[Mannose]_O$= 0.02 M.

T [°K]	10^3 1/T	10^5 k_2 [L·mol^{-1}·sec^{-1}]	ln k_2	5+log k_2
333	3.000	4.53	-10.0022	0.6561
343	2.915	10.70	-9.1427	1.02938
348	2.874	16.24	-8.7254	1.2107
353	2.833	36.08	-7.9271	1.55724

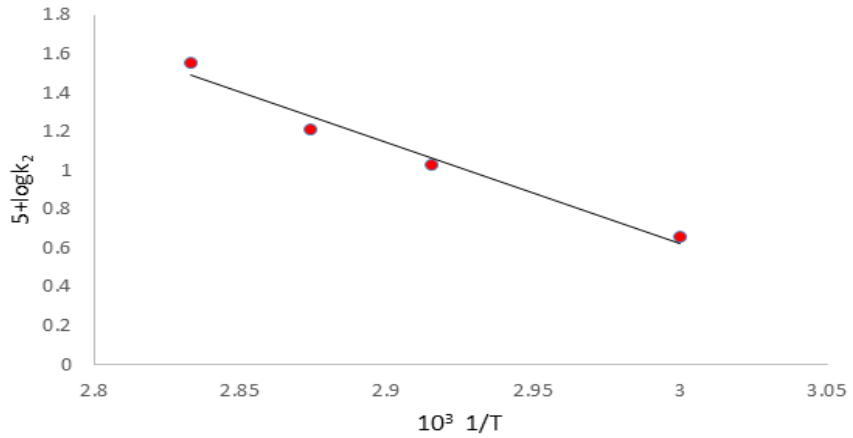

Figure 11. Evaluation of the activation energy of the bimolecular reaction from k_2 over the range of 60-80°C.

The bimolecular reaction's activation energy is determined to be 23.66 kcal from the slope of the straight line that resulted from plotting log k_2 versus 1/T (Fig. 11, Table 15). The activation energy of the mannose-peroxydisulfate i.e., the overall reaction including thermal decomposition was found to be 26.85 kcal, this value falls intermediate between that for the thermal decomposition alone 28.70 kcal [81] and that for the bimolecular reaction between mannose and peroxydisulfate.

Proposed Mechanism and the Rate Law

The mannose-peroxydisulfate reaction produced two fractions: one volatile, consisting of formaldehyde and formic acid, and the other non-volatile, or residue, which mostly included potassium hydrogen sulfate, aldonic and aldaric acids, and other oxidation products. Based on these two truths, it is obvious that three paths exist in the mannose-peroxydisulfate reaction, as shown by the following rate law: one term represents thermal breakdown alone, and the second term represents the bimolecular reaction. The formation of these products represents the oxidation by peroxydisulfate of the terminal groups in the mannose molecule and the C-C oxidative cleavage:

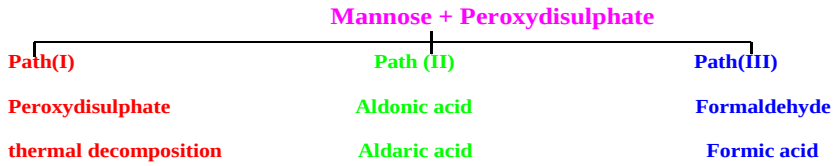

Path (I) can be represented in the following manner**:**

$$S_2O_8 \xrightarrow{k_1} 2SO_4^- \quad (8)$$

$$SO_4^- + H_2O \xrightarrow{k_2} HSO_4^- + OH^- \quad (9)$$

$$2OH^- \xrightarrow{k_2} H_2O + \frac{1}{2}O_2 \quad (10)$$

In pathway (II), aldonic and aldaric acids are produced. The subsequent process leads to the production of aldonic acid as a result of direct oxidation of the aldehydic group found terminal in the mannose molecule:

$$RCHO + SO_4^- \xrightarrow{k_3} R - C = O + HSO_4^- \quad (11)$$

$$R - C = O + H_2O \xrightarrow{k_4} RCOOH + H^\bullet \quad (12)$$

$$H^\bullet + OH^\bullet \xrightarrow{k_5} H_2O \quad (13)$$

The following steps are involved in the creation of aldaric acid as a result of oxidation of the principal alcoholic group found in the mannose molecule:

$$RCH_2OH^\bullet \xrightarrow{k_6} RCHOH + H_2O \quad (14)$$

$$RCHOH + S_2O_8 = \xrightarrow{k_7} RCHO + HSO_4^- + SO_4^- \quad (15)$$

$$RCHOH + SO_4^- = \xrightarrow{k_8} RCHO + HSO_4^- \quad (16)$$

In conclusion, it can consider the formation of formaldehyde and formic acid through path (III) since no product with 2, 3, 4, or 5 carbon atoms can be isolated, it can be inferred that the C-C oxidative splitting process continues until the mannose molecule is entirely transformed into formaldehyde and formic acid. The following scheme is designed to illustrate the formation of such products:

$$CHO \cdot (CHOH)_4 \cdot CH_2OH + OH^\bullet \longrightarrow CHO \cdot (CHOH)_4 \cdot CHOH + H_2O \quad (17)$$

$$CHO \cdot (CHOH)_4 \cdot CHOH \longrightarrow CHO \cdot (CHOH)_4 + HCHO \quad (18)$$

$$CHO \cdot (CHOH)_4 + SO_4^\bullet \longrightarrow CHO(CHOH)_3 + CHO + HSO_4 \quad (19)$$

$$CHO \cdot (CHOH)_3 + SO_4^\bullet \longrightarrow CHO(CHOH)_2 + CHO + HSO_4 \quad (20)$$

If this scheme from 10 to 13 continuous one mannose molecule produces five CHO radicals, which in turn produce formic acid.

$$5CHO + 5OH^\bullet \longrightarrow 5HCOOH \quad (21)$$

Following this procedure should result in the production of five formic acid molecules and one formaldehyde molecule for every oxidized mannose molecule. Implementing the steady state approach to pathways (I) and (II) simplifies the task of trying to connect the observed rate law Equation (3) with the suggested mechanism Equations (8) to (21).

The following equation represents the rate of disappearance of peroxydisulfate in a steady state:

$$-\frac{d[S_2O_8^{=}]}{dt} = k_1[S_2O_8^{=}] + k_7[RCHOH][S_2O_8^{=}] \quad (22)$$

The following equations indicate the zero rate of change in the concentration of the radicals (RCHOH), (SO_4^-), (OH), (H), and (R-C = O) with respect to time.:

$$\frac{d[R.CHOH]}{dt} = \mathbf{k_6}[RCH_2OH][OH] - \mathbf{k_7}[RCHOH][S_2O_8^{=}] - \mathbf{k_8}[RCHOH][SO_4^-] = 0$$

$$\mathbf{k_6}[\text{Mannose}][OH] = \mathbf{k_7}[RCHOH][S_2O_8^{=}] + \mathbf{k_8}[RCHOH][SO_4^-] \quad \mathbf{(A)}$$

$$\frac{d[SO_4^-]}{dt} = \mathbf{k_1}[S_2O_8^{=}] - \mathbf{k_2}[SO_4^-][H_2O] - \mathbf{k_3}[RCHO][SO_4^-] + \mathbf{k_7}[RCHOH][S_2O_8^{=}] - \mathbf{k_8}[RCHOH][SO_4^-] = 0$$

$$\mathbf{k_1}[S_2O_8^{=}] + \mathbf{k_7}[RCHOH][S_2O_8^{=}] = \mathbf{k_2}[SO_4^-][H_2O] + \mathbf{k_3}[\text{Mannose}][SO_4^-] + \mathbf{k_8}[RCHOH][SO_4^-] \quad \mathbf{(B)}$$

$$\frac{d[OH]}{dt} = \mathbf{k_2}[SO_4^-][H_2O] - \mathbf{k_5}[H][OH] - \mathbf{k_6}[RCH_2OH][OH] = 0$$

$$\mathbf{k_2}[SO_4^-][H_2O] = \mathbf{k_5}[H][OH] + \mathbf{k_6}[\text{Mannose}][OH] \quad \mathbf{(C)}$$

$$\frac{d[H]}{dt} = \mathbf{k_4}[R\text{-}C{=}O][H_2O] - \mathbf{k_5}[H][OH] = 0$$

$$\mathbf{k_4}[R\text{-}C{=}O][H_2O] = \mathbf{k_5}[H][OH] \quad \mathbf{(D)}$$

$$\frac{d[R\text{-}C = O]}{dt} = \mathbf{k_3}[RCHO][SO_4^-] - \mathbf{k_4}[R\text{-}C = O][H_2O] = 0$$

$$\mathbf{k_3}[\text{Mannose}][SO_4^-] = \mathbf{k_4}[R\text{-}C = O][H_2O] \quad \mathbf{(E)}$$

We may write equation (C) as follows using Equations (D) and (E) as inputs:

$$\mathbf{k_2}[SO_4^-][H_2O] = \mathbf{k_3}[\text{Mannose}][SO_4^-] + \mathbf{k_6}[\text{Mannose}][OH] \quad \mathbf{(F)}$$

After plugging the k_6[Mannose] [OH] value from (F) into (A), was obtained**:**

$$\mathbf{k_2}[SO_4^-][H_2O] - \mathbf{k_3}[\text{Mannose}][SO_4^-] = \mathbf{k_7}[RCHOH][S_2O_8^{=}] + \mathbf{k_8}[RCHOH][SO_4^-] \quad \mathbf{(G)}$$

It is possible to rewrite Equation (G) so that it becomes**:**

$$\mathbf{k_7}[RCHOH][S_2O_8^{=}] = [SO_4^-]\left[\mathbf{k_2}[H_2O] - \mathbf{k_3}[\text{Mannose}] - \mathbf{k_8}[RCHOH]\right] \quad \mathbf{(H)}$$

We may express equation (B) in the following way:

$$[S_2O_8^{=}]\left[\mathbf{k_1} + \mathbf{k_7}[RCHOH]\right] = [SO_4^-]\left[\mathbf{k_2}[H_2O] + \mathbf{k_3}[\text{Mannose}] + \mathbf{k_8}[RCHOH]\right] \quad \mathbf{(I)}$$

On dividing equation **(I)** by equation **(H)** we get**:**

$$[S_2O_8^{=}]\frac{[\mathbf{k_1}+\mathbf{k_7}\,[RCHOH]]}{\mathbf{k_7}\,[RCHOH]\,[S_2O_8^{=}]} = \frac{\mathbf{k_2}\,[H_2O]+\mathbf{k_3}\,[Mannose]+\mathbf{k_8}\,[RCHOH]}{\mathbf{k_2}\,[H_2O]-\mathbf{k_3}\,[Mannose]-\mathbf{k_8}\,[RCHOH]} \quad \textbf{(J)}$$

By Cross- multiplication of the sides in equation **(J)** and rearranging we get:

$$2\,\mathbf{k_7}\,\mathbf{k_8}\,[RCHOH]^2 + [RCHOH]\left[2\,\mathbf{k_3}\,\mathbf{k_7}\,[Mannose]+\mathbf{k_1}\,\mathbf{k_8}\right]+\mathbf{k_1}\,\mathbf{k_3}\,[Mannose]-\mathbf{k_1}\mathbf{k_2}\,[H_2O]=0 \quad \textbf{(K)}$$

or

$$\mathbf{[RCHOH]^2} + \frac{\left[2\,\mathbf{k_3}\,\mathbf{k_7}\,[Mannose]+\mathbf{k_1}\,\mathbf{k_8}\right]}{2\,\mathbf{k_7}\,\mathbf{k_8}}\mathbf{[RCHOH]} + \frac{\left[\mathbf{k_1}\,\mathbf{k_3}\,[Mannose]-\mathbf{k_1}\mathbf{k_2}\,[H_2O]\right]}{2\,\mathbf{k_7}\,\mathbf{k_8}} = 0 \ \textbf{(L)}$$

On solving equation **(L)** for **[RCHOH]**, we get**:**

$$\mathbf{[RCHOH]} = -\frac{2\,\mathbf{k_3}\,\mathbf{k_7}\,[Mannose]+\mathbf{k_1}\,\mathbf{k_8}}{2\,\mathbf{k_7}\,\mathbf{k_8}} + \mathbf{1/2}\sqrt{\left(\frac{2\,\mathbf{k_3}\,\mathbf{k_7}\,[Mannose]+\mathbf{k_1}\,\mathbf{k_8}}{2\,\mathbf{k_7}\,\mathbf{k_8}}\right)^2 - 4\,\frac{\mathbf{k_1}\,\mathbf{k_3}\,[Mannose]-\mathbf{k_1}\mathbf{k_2}\,[H_2O]}{2\,\mathbf{k_7}\,\mathbf{k_8}}} \quad \textbf{(M)}$$

If we substitute the value of **[RCHOH]** in equation **(**22**)** for the rate law we get**:**

$$-\frac{d[S_2O_8^{=}]}{dt} = \mathbf{k_1}[S_2O_8^{=}] - \mathbf{k_7}\left[2\,\frac{\mathbf{k_3}\,\mathbf{k_7}\,[Mannose]+\mathbf{k_1}\,\mathbf{k_8}}{2\,k_7\,k_8} + 1/2\sqrt{\left[2\,\frac{\mathbf{k_3}\,\mathbf{k_7}\,[Mannose]+\mathbf{k_1}\,\mathbf{k_8}}{2\,k_7\,k_8}\right]^2 - 4\,\frac{\mathbf{k_1}\,\mathbf{k_3}\,[Mannose]-\mathbf{k_1}\mathbf{k_2}\,[H_2O]}{2\,k_7\,k_8}}\right]\mathbf{[S_2O_8^{=}]} \quad \textbf{(N)}$$

$$= \mathbf{k_o}[S_2O_8^{=}]$$

where

$$\mathbf{k_o} = \mathbf{k_1} - \mathbf{k_7}\left[2\,\frac{\mathbf{k_3}\,\mathbf{k_7}\,[Mannose]+\mathbf{k_1}\,\mathbf{k_8}}{2\,k_7\,k_8} + 1/2\sqrt{\left[2\,\frac{\mathbf{k_3}\,\mathbf{k_7}\,[Mannose]+\mathbf{k_1}\,\mathbf{k_8}}{2\,k_7\,k_8}\right]^2 - \frac{4\,\mathbf{k_1}\,\mathbf{k_3}\,[Mannose]-\mathbf{k_1}\mathbf{k_2}\,[H_2O]}{2\,k_7\,k_8}}\right]$$

4. CONCLUSIONS

According to the results of this research, peroxydisulfate is a great oxidant for mannose molecules because it oxidizes the aldehydic and primary alcoholic groups and causes oxidative breakage of the C-C bonds. Oxidation exhibits properties of chain reactions due to its free-radical chain mechanism, which is responsible for the following: When it comes to peroxydisulfate, the reaction is first order, and when it comes to mannose concentration, it's fractional order. No change in temperature affects the sequence of this reaction. When it comes to surface effect, both the rate and the rate constant are quite

sensitive. Thermal decomposition of peroxydisulfate releases sulfate free radicals (SO_4^-), which can be neutralized by reacting with water to form oxygen or by combining with mannose molecules to form free radicals that attack peroxydisulfate; this explains why adding mannose accelerates the decomposition rate of peroxydisulfate.In a typical mathematical expression of the temperature effect on the reaction, two parameters are introduced (Fig. 9): the intercept, which is the frequency factor (A) and is found to be $1.6X10^{-5}sec^{-1}$, and the slope of the straight line, which is the activation energy Ea and is found to be 26.85 kcal/mole. Table 1 displays the outcomes of the activation functions, change in entropy (ΔS#), and change in free energy (ΔG#). A strong electrostatic contact between the solute and solvent is suggested by the positive value of the free energy of activation, which is further reinforced by the negative value of ΔS#, which indicates the solvated intermediate state. The existence of heavily solvated transition intermediate states is indicated by a negative activation entropy value, whereas sluggish kinetics is suggested by a negative activation energy value. A rate law was derived using the mechanism proposed for the mannose-peroxydisulfate reaction.

Acknowledgment: *The author extends his appreciation to the Deanship of Scientific Research at Northern Border University, Arar, KSA for funding this research work through the project number "NBU-FFR-2024-800-0X"*

REFERENCES

[1] Singh, A.K., Chopram, D., Rahmanim, S., Singh, B., *Carbohydrates Research*, **314**, 151, 1998.
[2] Hanover, L.M., White, J.S., *Journal of Clinical Nutrition*, **58**, 724, 1993.
[3] Singh, A.K., Srivastava, J., Rahmani, S., *Journal of Molecular Catalysis A: Chemical*, **271**, 151, 2007.
[4] Tripathi, R., Upadhyay, S.K., *International Journal of Chemical Kinetics*, **36,** 441, 2004.
[5] Dash, S., Patel, S., Mishra, B.K, *Tetrahedron*, **65**, 707, 2009.
[6] Ruhoof, J.R., *Organic Syntheses*, **2**, 315, 1943.
[7] Odebunmi, E.O., Iwarere, S.A., Owalude, S.O., *International Journal of Chemistry*, **16**(3), 167, 2006.
[8] Odebunmi, E. O., Obike, A.I., Owalude, S. O., *International Research Journal of Biochemistry and Bioinformatics*, **2**(2), 122, 2009.
[9] Odebunmi, E. O., Ogunlaja, A. S., Owalude, S. O., *Orbital Electronic Journal of Chemistry* **2**(2),127, 2010.
[10] Sheltar, R.S., Hiremath, M.I., Nandibewoor, S.T., *E-Journal of Chemistry*, **2**(6), 91, 2005.
[11] Hiremath, G.A., Timmanagoudar, P.L., Nandibewoor, S.T. *Transition Metal Chemistry*, **21**(6), 560, 1996.
[12] Abualreish, M.J.A., *Asian Journal of Chemistry*, **21**(6)**,** 4162, 2009.
[13] Abualreish, M.J.A., Aissa, A., *International Journal of Basic and Applied Sciences*, **4**(1), 121, 2015.
[14] Abualreish, M.J.A., *Research Journal of Chemistry and Environment*, **22**(7), 12, 2018.
[15] Abualreish, M.J.A., *Scientific Study and Research Chemistry and Chemical Engineering, Biotechnology, Food Industry*, **24**(2), 081, 2023.
[16] Abualreish, M.J.A., *Journal of Physical Science*, **34**(3), 21, 2023**.**
[17] Srivastava, S., Srivastava, P., Chaudhary, L., Kumar, A., Singh, S., *Journal of the Indian Chemical Society*, **86**, 58, 2009.
[18] Goel, A. *Journal of the Indian Chemical Society*, **85**(3), 286-289.2008

[19] Rajput, S.K., Sharma, A., *Journal of the Indian Chemical Society*, **85**, 71, 2008.
[20] Okoro, H.K., Odebunmi, E.O., *International Journal of Physical Sciences*, **4**(9), 471, 2009.
[21] Odebunmi, E.O., Owalude, S.O., *Journal of the Iranian Chemical Society*, **5**(4), 23, 2008.
[22] Grgur, B.N., Žugić, D.L., Gvozdenović, M.M., Trišović, T.L. *Carbohydrate research*, **341**(11), 1779, 2006
[23] Singh, A. K., Chaurasia, N., Rahmani, S., Srivastava, J., & Singh, A. K.. *Journal of Chemical Research*, **2005**(5), 304, 2005.
[24] Singh, A. K., Reena, R., Jaya, S., Shahla, R., Shalini, S., *Journal of Organometallic Chemistry*, **692**(20), 4270, 2007.
[25] Singh, A. K., Shalini, S., Jaya, S., Srivastava, R., Singh, P., *Journal of Molecular Catalysis A: Chemical*, **278**(1-2), 72, 2007.
[26] Singh, A.K., Chaurasia, N., Jaya, S., Shahla, R., Singh, B., *Catalysis Letters*, **95**(3-4), 135, 2004.
[27] Singh, A.K., Singh, V., Singh, A.K., Gupta, N., Singh, B., *Carbohydrate Research*, **337**(4), 345, 2002.
[28] Roldán, V., Carlos González, J., Santoro, M., García, S., Casado, N., Olivera, S., Sala, L.F. *Canadian journal of chemistry*, **80**(12), 1676, 2002.
[29] Sussich, F., Cesaro, A., *Carbohydrate Research*, **329**(1), 87, 2000.
[30] Odebunmi, E.O., Oyetunj, O.A., Marufu, H., *Nigerian Journal of Science*, **33**, 145, 1999.
[31] Reddy, K.N., Reddy, M.K.R., Rajanna, K.C., *Transition Metal Chemistry*, **21**, 112, 1996.
[32] Varadarajan, R., Dhar, R.K., *Indian Journal of Chemistry*, **25**(A)**,** 339, 1986.
[33] Srivastava, R.K., Nath, N., Singh, M.P., *Bulletin of the Chemical Society of Japan*, **39**(4), 833, 1966.
[34] Lee, C., Kim, H.H., Park, N.B., *Membrane Water Treatment*, **9**(6), 405**,** 2018.
[35] Tsitonaki, A., Petri, B., Crimi, M., Mosbaek, H., Siegrist, R.L., Bjerg, P.L, *Critical Reviews in Environmental Science and Technology*, **40**(1), 55, 2010.
[36] Matzek, L.W., Carter, K.E., *Chemosphere*, **151**, 178, 2016.
[37] Zhao, Q.X., Mao, Q.M., Zhou, Y.Y., Wei, J.H., Liu, X.C., Yang, J.Y., Luo, L., Zhang, J.C., Chen, H., Chen, H.B., Tang, L, *Chemosphere*, **189**, 224, 2017.
[38] Wacławek, S., Lutze, H.V., Grubel, K., Padil, V.V.T., Cernik, M., Dionysiou, D.D., *Chemical Engineering Journal*, **330**, 44, 2017.
[39] Ike, I.A., Linden, K.G., Orbell, J.D., Duke, M., *Chemical Engineering Journal*, **338**, 651, 2018.
[40] Wang, J.L., Wang, S.Z., *Chemical Engineering Journal*, **334**, 1502, 2018.
[41] Huang, K.C., Couttenye, R.A., Hoag, G.E., *Chemosphere*, **49**, 413, 2002.
[42] Anipsitakis, G.P., Dionysiou, D.D., *Environmental Science and Technology Journal*, **38**, 3705, 2004.
[43] Liang, C., Bruell, C.J., Marley, M.C., Sperry, K.L., *Chemosphere*, **55,** 1225, 2004.
[44] Waldemer, R.H., Tratnyek, P.G., Johnson, R.L., Nurmi, J.T, *Environmental Science and Technology Journal*, **41**, 1010, 2007.
[45] Liang, C., Huang, C.F., Chen, Y.J., *Water Research*, **42**, 4091, 2008.
[46] Eberson, L., Ekstrom, M., *Acta Chemica Scandinavica*, **B41**, 41, 1987.
[47] Latimer, W.M., *The Oxidation States of the Elements and Their Potentials in Aqueous Solutions*, 2nd Edition New York, Prentice Hall, p. 392, 1952.
[48] Gucker, F.T., *Journal of Chemical Education*, **17**(8), 401, 1940.
[49] Kolthoff, I.M., Carr, E. M., *Analytical Chemistry Journal*, **25**(2), 298, 1953.
[50] Wahba, N., El Asmar, M.F., El Sadr, M.M., *Analytical Chemistry Journal*, **31**(11), 1870, 1959.

[51] Amin, D., Hareez, A. K., *Analyst*, **106**, 1221, 1981.
[52] Belcher, R., *Talanta*, **15**(4)**,** 357, 1968.
[53] Frigerio, N. A., *Analytical Chemistry Journal*, **35**(3), 412, 1963.
[54] Leipert, T., *Mikrochemie*, **7**(S1), 266, 1929.
[55] Hakoila, E., *Talanta*, **15**(1), 55, 1968.
[56] Kolthoff, I. M., Woods, R., *Journal of the American Chemical Society*, **88**(7), 1371, 1966.
[57] Belcher, R., Bogdanski, S. L., Knowles, D. J., Townshend, A., *Analytica Chimica Acta*, **77**, 53, 1975.
[58] Laser, D., Bard, A. J., *Journal of the Electrochemical Society*, **122**, 632, 1975.
[59] Poznyak, S. K., Kulak, A. I., *Talanta*, **43**(9), 1607, 1996.
[60] Velasco, J. G., *Electroanalysis*, **3**(4-5), 261, 1991.
[61] White, H.S., Bard, A.J., *Journal of the American Chemical Society*, **104**(25), 6891, 1982.
[62] Xu, G., Dong, S., *Analytica Chimica Acta*, **412**(1-2), 235, 2000.
[63] Yamashita, K., Yamazaki-Nishida, S., Harima, Y., Segawa, A., *Analytical Chemistry Journal*, **63**(9), 872, 1991.
[64] Oliveira, M., Saczk, A., Neto, J., Roldan, P., Stradiotto, N., *Sensors*, **33**(9), 371, 2003.
[65] Lin, K.C., Huang, J.Y., Chen, S.M., *International Journal of Electrochemical Science*, **7**, 9161, 2012.
[66] Savari, Z., Soltanian, S., Noorbakhsh, A., Salimi, A., Najafi, M., Servati, P., *Sensors and Actuators*, 176, 335, 2013.
[67] Weibenbacher, M., Kalcher, K., Greschonig, H., Ng, W., Chan, W.H., Voulgaropoulos, A., *Journal of Analytical Chemistry*, **344**(3), 87, 1992.
[68] Gokulakrishnan, S., Mohammed, A., Prakash, H., *Chemical Engineering Journal*, **286**, 223, 2016.
[69] Zhao, L., Yang, S., Wang, L., Shi, C., Huo, M., Li, Y., *Journal of Environmental Sciences*, **31**, 235, 2015.
[70] Zou, J., Ma, J., Zhang, X., Xie, P., *Chemical Engineering Journal*, **253**, 34, 2014.
[71] Badekar, P.S., Kumbhar, A.A., *New Journal of Chemistry*, **42**(5), 3917, 2018.
[72] Huang, G.X., Si, J.Y., Qian, C., Wang, W.K., Mei, S.C., Wang, C.Y., Yu, H.Q., *Analytical Chemistry Journal*, **90**(24), 14439, 2018.
[73] Qasem, M., Kurdi, R. E., Patra, D., *Microchemical Journal*, **155**, 104701, 2020.
[74] Baalbaki, A., Eddine, N. Z., Jaber, S., Amasha, M., Ghauch, A., *Talanta*, **178**, 237, 2018.
[75] Huang, Z., Ni, C., Wang, F., Zhu, Z., Subhani, Q., Wang, M., Zhu, Y., *Journal of Separation Science*, **37,** 3198, 2014.
[76] Khan, N.E., Adewuyi, Y.G., *Journal of Chromatography A*, **1218**(3), 392, 2011.
[77] Weidenauer, M., Hoffmann, P., Lieser, K.H., *Fresenius Zeitschrift FürAnalytische Chemie*, **331**, 372, 1988.
[78] Weidenauer, P. Hoffmann, K., Lieser, H., *Fresenius' Journal of Analytical Chemistry*, **342**(4-5), 333, 1992.
[79] Abualreish, M. J. A., *Research Journal of Chemistry and Environment*, **25**(3), 142, 2021.
[80] Shuchi, S.B., Suhan, M.B.K., Bin-Humayun, S., Haque, M.E., Islam, M.S., *Journal of Water Process Engineering*, **39**, 101690, 2021.
[81] Ghauch, A., Tuqan, A. M., *Chemical Engineering Journal*, **183**, 162, 2012.
[82] Ahmadi, S., Igwegbe, C. A., Rahdar, S., *International Journal of Industrial Chemistry*, **10**, 249, 2019.
[83] Vasudeva, W. C., Wasif, S., *Journal of the Chemical Society*, (B), 960, 1970.
[84] Ahmadi, S., Igwegbe, C. A., Rahdar, S., *International Journal of Industrial Chemistry*, **10,** 249, 2019.